Phosphorus driven embrittlement and atomistic crack behavior in tungsten grain boundaries: Supplementary material

S1. COMPUTATION OF AVERAGED ENERGY RELEASE RATE

The average energy release rate, G_I, is calculated by averaging the G_I^{CZ} values of five CZVEs. The G_I for all the considered STGBs with varying P impurity coverage, θ, is provided in Table S1.

Table S1. Averaged energy release rate (G_I in units of Jm^2) of the $\langle 110 \rangle$ STGBs considered in the present work. Here, 'pr.dir' is short for crack propagation direction and θ stands for P impurities coverage.

GB, crack system	G_I			
Σ/[pr.dir]	$\theta = 0.0$ Å^{-2}	$\theta = 0.02$ Å^{-2}	$\theta = 0.04$ Å^{-2}	$\theta = 0.06$ Å^{-2}
$\Sigma 51/[5\bar{5}\bar{1}]$	5.83	5.78	4.82	4.07
$\Sigma 3(\bar{1}12)/[\bar{1}1\bar{1}]$	6.96	6.33	6.27	6.51
$\Sigma 17(2\bar{2}\bar{3})/[\bar{3}3\bar{4}]$	5.93	5.24	4.65	3.90
$\Sigma 17(3\bar{3}\bar{4})/[2\bar{2}3]$	5.53	5.18	4.64	4.10
$\Sigma 43/[3\bar{3}5]$	5.61	5.32	4.90	3.80
$\Sigma 3(1\bar{1}\bar{1})/[1\bar{1}2]$	5.54	5.03	4.49	3.92
$\Sigma 11/[\bar{2}2\bar{5}]$	5.84	5.36	4.34	3.55
$\Sigma 9/[1\bar{1}4]$	5.53	4.84	4.52	3.88
$\Sigma 27/[\bar{1}1\bar{5}]$	4.89	5.24	4.78	4.52
$\Sigma 19/[\bar{1}1\bar{6}]$	4.68	4.56	4.23	4.05
$\Sigma 33/[1\bar{1}\bar{8}]$	4.77	4.81	4.27	3.92

S2. CRACK GROWTH RESISTANCE (R)-CURVES FOR ALL THE STGBS

The R-curves for all STGBs are presented in Figures S1 and S2. R-curves are obtained by plotting the data of crack growth, Δa_{crack}, versus applied K_I i.e. K_I term in the LEFM anisotropic displacement fields [1–4], given by

$$u_x = K_I\sqrt{\frac{2r}{\pi}}\Re\left\{\left[\frac{1}{(\mu_1-\mu_2)}\right]\left[\mu_1 p_2(\cos\theta+\mu_2\sin\theta)^{1/2}-\mu_2 p_1(\cos\theta+\mu_1\sin\theta)^{1/2}\right]\right\}, \quad \text{(S1)}$$

$$u_y = K_I\sqrt{\frac{2r}{\pi}}\Re\left\{\left[\frac{1}{(\mu_1-\mu_2)}\right]\left[\mu_1 q_2(\cos\theta+\mu_2\sin\theta)^{1/2}-\mu_2 q_1(\cos\theta+\mu_1\sin\theta)^{1/2}\right]\right\}, \quad \text{(S2)}$$

where,

$$p_1 = s_{11}\mu_1^2 + s_{12} - s_{16}\mu_1 \quad \text{(S3)}$$

$$p_2 = s_{11}\mu_2^2 + s_{12} - s_{16}\mu_2, \quad \text{(S4)}$$

$$q_1 = \frac{s_{12}\mu_1^2 + s_{22} - s_{26}\mu_1}{\mu_1}, \quad \text{(S5)}$$

$$q_2 = \frac{s_{12}\mu_2^2 + s_{22} - s_{26}\mu_2}{\mu_2}. \quad \text{(S6)}$$

Here, μ_1 and μ_2 are the complex solutions of the characteristic equation,

$$s_{11}\mu_j^4 - 2s_{16}\mu_j^3 + (2s_{12}+s_{66})\mu_j^2 - 2s_{26}\mu_j + s_{22} = 0. \quad \text{(S7)}$$

The s_{ij}s are the compliance constants at 0 K, in the orientation of interest.

S3. COMPUTATION OF FRACTURE TOUGHNESS

Table S2. Fracture toughness (K_{IC}^{R} in units of MPa·m$^{1/2}$) of the ⟨110⟩ STGBs considered in the present work. Here, 'pr.dir' is short for crack propagation direction and θ stands for P impurities coverage.

GB, crack system	K_{IC}^{R}			
Σ/[pr.dir]	θ = 0.0 Å^{-2}	θ = 0.02 Å^{-2}	θ = 0.04 Å^{-2}	θ = 0.06 Å^{-2}
$\Sigma 51/[5\bar{5}\bar{1}]$	1.18	1.58	1.36	0.875
$\Sigma 3(\bar{1}12)/[\bar{1}1\bar{1}]$	1.65	1.72	1.50	1.53
$\Sigma 17(2\bar{2}\bar{3})/[\bar{3}3\bar{4}]$	1.46	1.36	1.25	1.22
$\Sigma 17(3\bar{3}\bar{4})/[2\bar{2}3]$	1.50	1.38	1.55	0.84
$\Sigma 43/[3\bar{3}5]$	1.44	1.32	1.22	0.96
$\Sigma 3(1\bar{1}\bar{1})/[1\bar{1}2]$	1.44	1.31	1.22	1.16
$\Sigma 11/[\bar{2}2\bar{5}]$	1.35	1.08	0.98	1.05
$\Sigma 9/[1\bar{1}4]$	1.51	0.96	1.15	0.98
$\Sigma 27/[\bar{1}1\bar{5}]$	1.34	1.28	1.32	1.42
$\Sigma 19/[\bar{1}1\bar{6}]$	1.55	1.73	1.58	0.91
$\Sigma 33/[1\bar{1}\bar{8}]$	1.38	1.33	1.31	0.91

Table S3. Fracture toughness (K_{IC} in units of MPa·m$^{1/2}$) of the ⟨110⟩ STGBs considered in the present work. Here 'pr.dir' is short for crack propagation direction and θ stands for P impurities coverage.

GB, crack system	K_{IC}			
Σ/[pr.dir]	θ = 0.0 Å^{-2}	θ = 0.02 Å^{-2}	θ = 0.04 Å^{-2}	θ = 0.06 Å^{-2}
$\Sigma 51/[5\bar{5}\bar{1}]$	1.61	1.602	1.463	1.345
$\Sigma 3(\bar{1}12)/[\bar{1}1\bar{1}]$	1.76	1.68	1.67	1.70
$\Sigma 17(2\bar{2}\bar{3})/[\bar{3}3\bar{4}]$	1.62	1.53	1.44	1.32
$\Sigma 17(3\bar{3}\bar{4})/[2\bar{2}3]$	1.57	1.52	1.44	1.35
$\Sigma 43/[3\bar{3}5]$	1.58	1.54	1.48	1.30
$\Sigma 3(1\bar{1}\bar{1})/[1\bar{1}2]$	1.57	1.50	1.41	1.32
$\Sigma 11/[\bar{2}2\bar{5}]$	1.58	1.54	1.39	1.26
$\Sigma 9/[1\bar{1}4]$	1.57	1.47	1.42	1.31
$\Sigma 27/[\bar{1}1\bar{5}]$	1.48	1.53	1.46	1.42
$\Sigma 19/[\bar{1}1\bar{6}]$	1.44	1.42	1.37	1.34
$\Sigma 33/[1\bar{1}\bar{8}]$	1.46	1.46	1.38	1.32

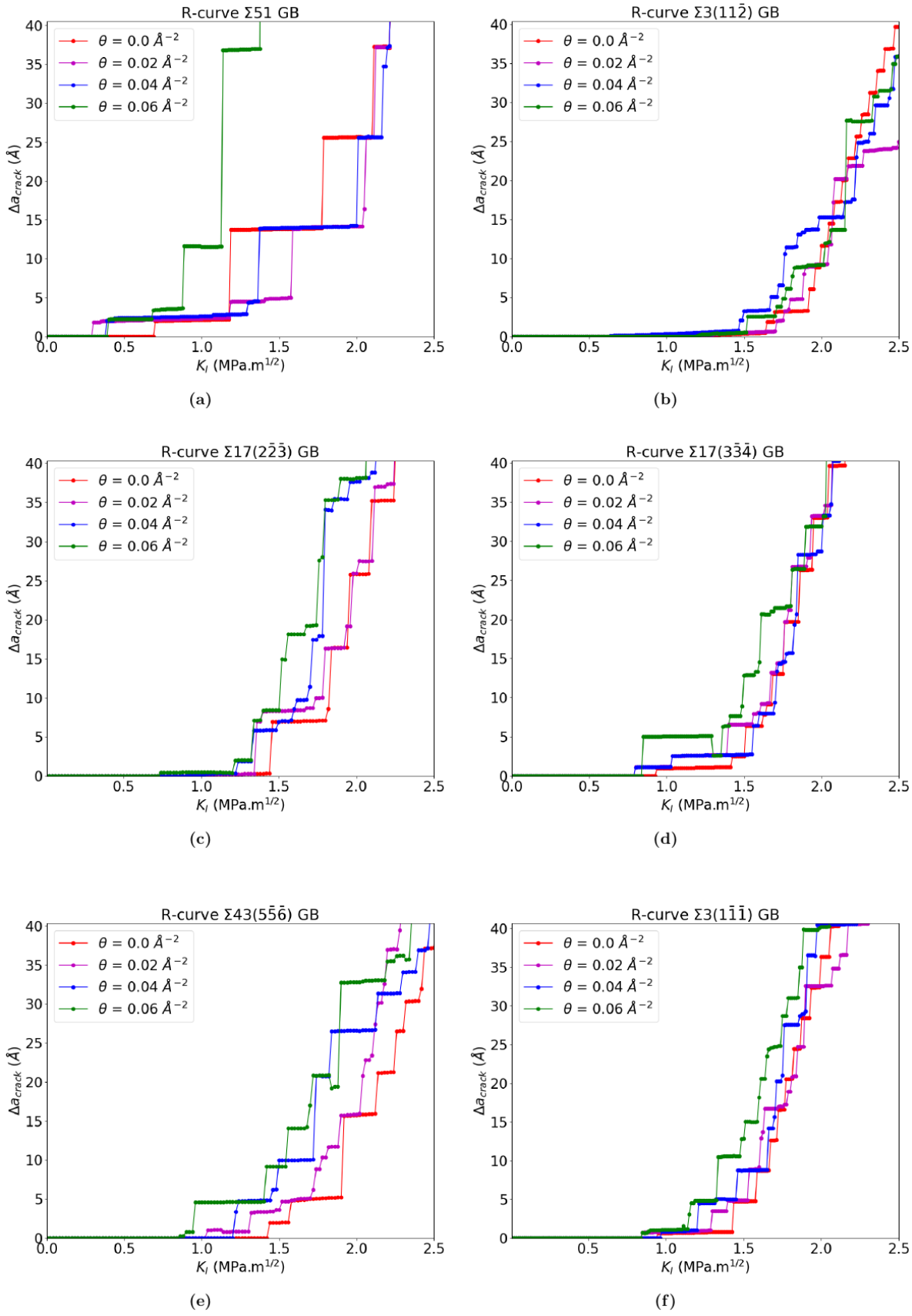

Fig. S1. *R*-curves for Σ51, Σ3($\bar{1}$12), Σ17(2$\bar{2}\bar{3}$), Σ17(3$\bar{3}\bar{4}$), Σ43 and Σ3(1$\bar{1}\bar{1}$) GB cracks.

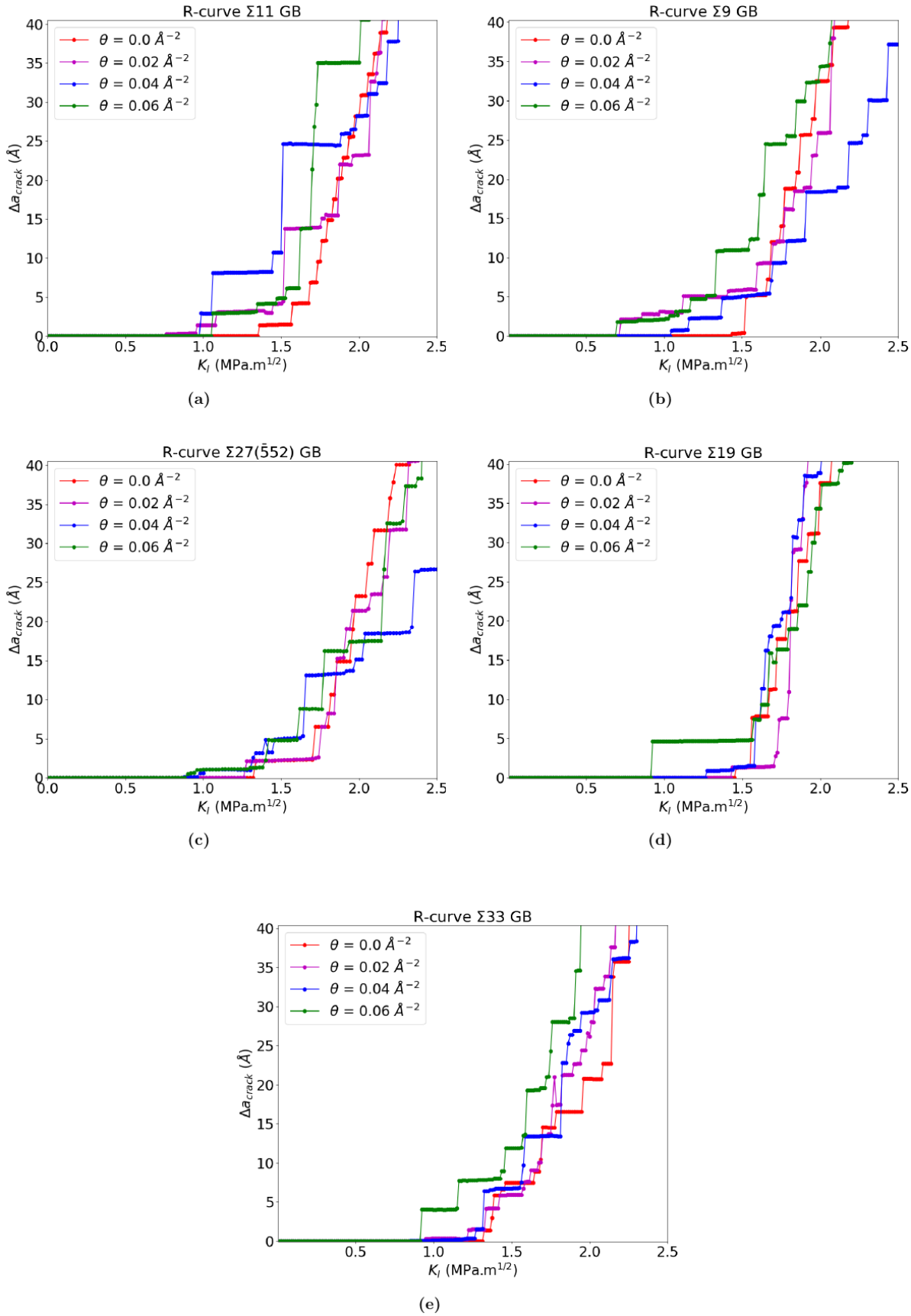

Fig. S2. *R*-curves for Σ11, Σ9, Σ27, Σ19 and Σ33 GB cracks.

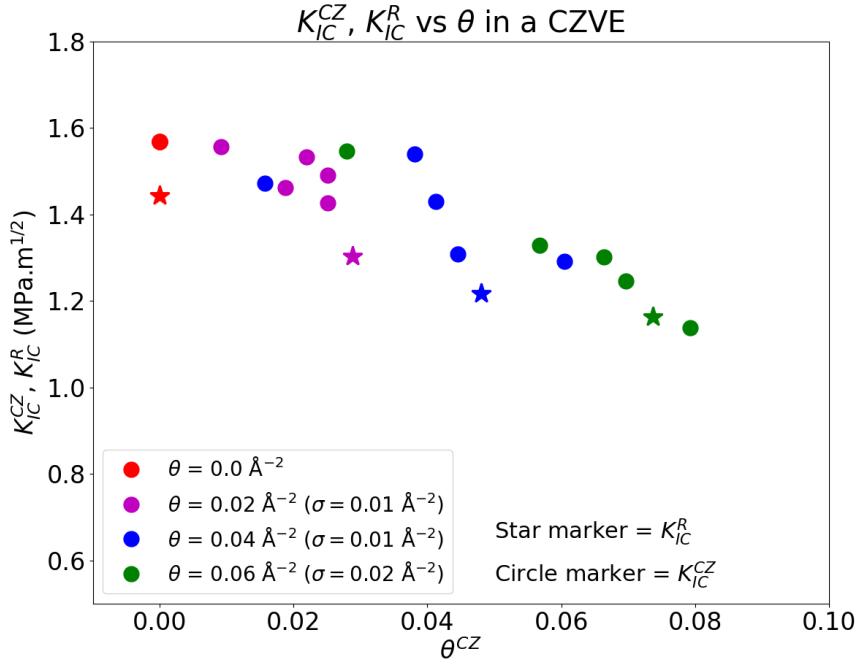

Fig. S3. K_{IC}^{CZ}-values in CZVEs of $\Sigma3(1\bar{1}\bar{1})$ GB cracks with varying impurity coverage, θ.

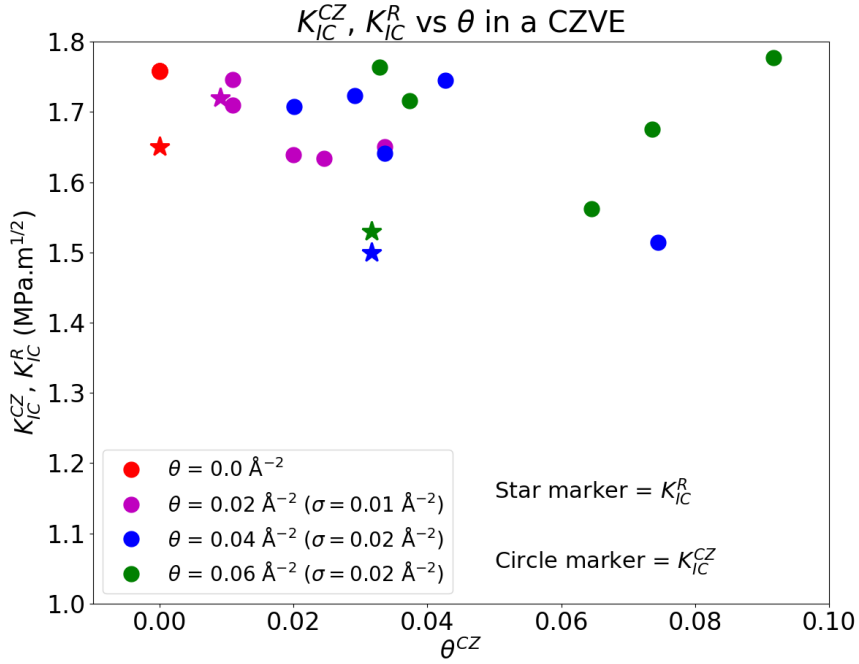

Fig. S4. K_{IC}^{CZ}-values in CZVEs of $\Sigma3(\bar{1}12)$ GB cracks with varying impurity coverage, θ.

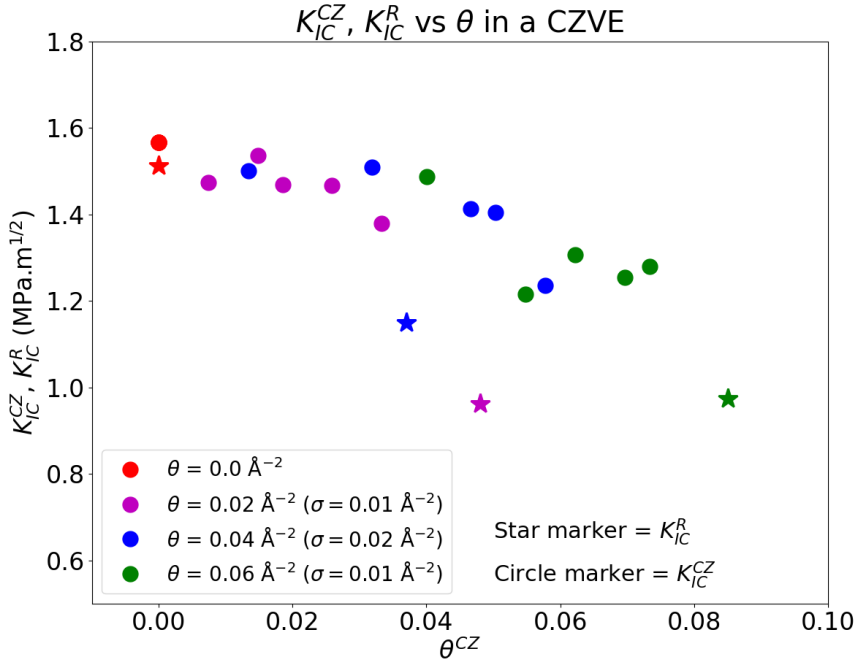

Fig. S5. K_{IC}^{CZ}-values in CZVEs of $\Sigma 9$ GB cracks with varying impurity coverage, θ.

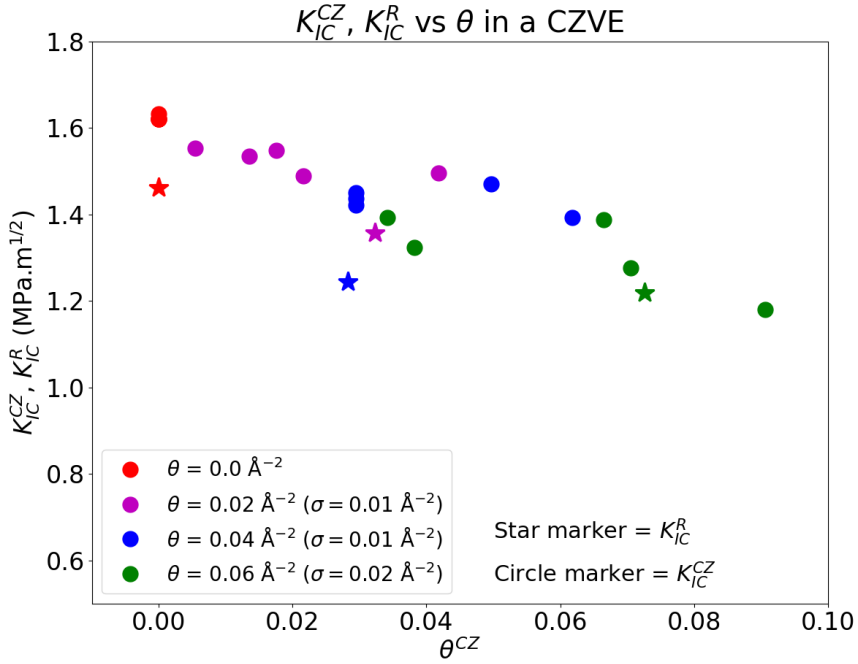

Fig. S6. K_{IC}^{CZ}-values in CZVEs of $\Sigma 17(2\bar{2}\bar{3})$ GB cracks with varying impurity coverage, θ.

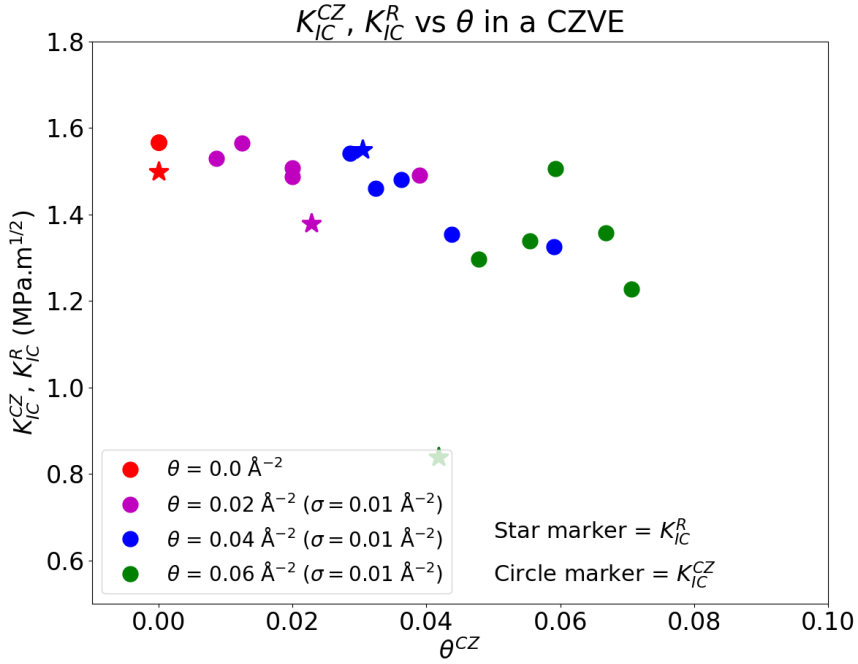

Fig. S7. K_{IC}^{CZ}-values in CZVEs of $\Sigma17(3\bar{3}\bar{4})$ GB cracks with varying impurity coverage, θ.

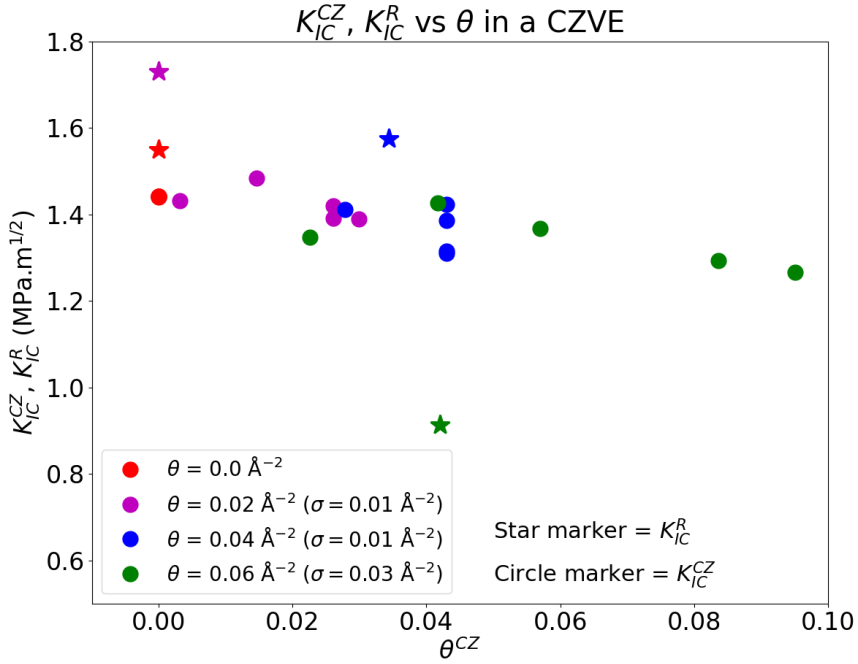

Fig. S8. K_{IC}^{CZ}-values in CZVEs of $\Sigma19$ GB cracks with varying impurity coverage, θ.

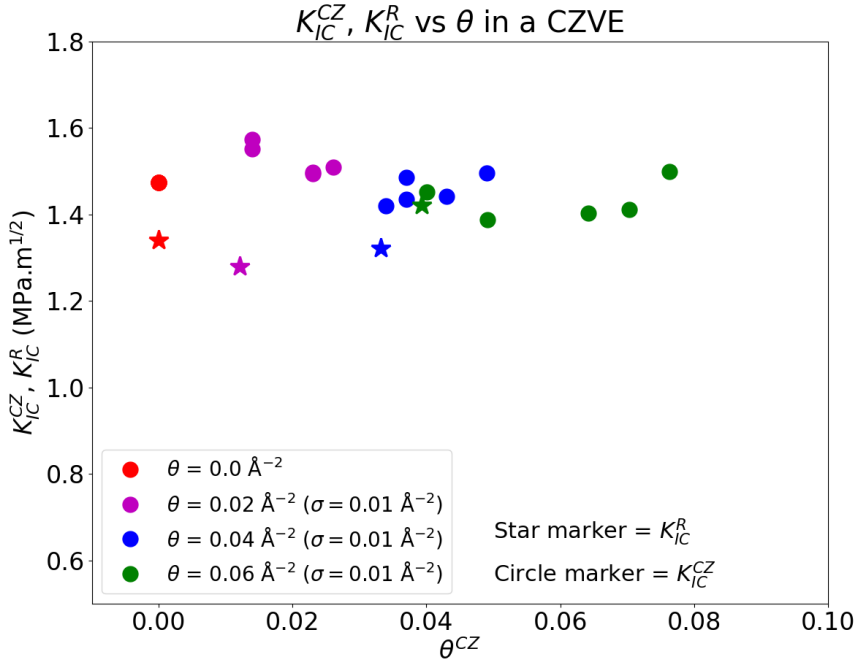

Fig. S9. K_{IC}^{CZ}-values in CZVEs of Σ27 GB cracks with varying impurity coverage, θ.

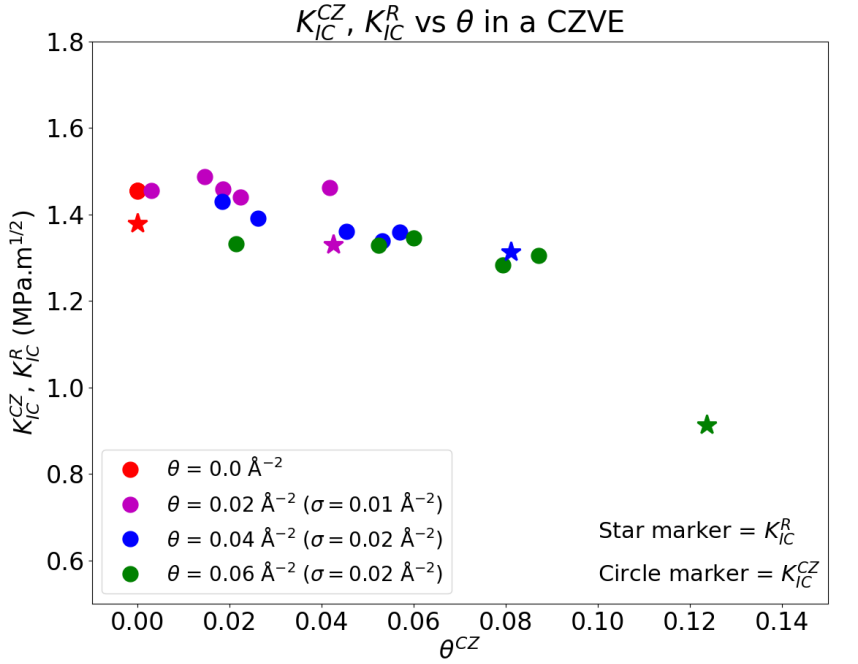

Fig. S10. K_{IC}^{CZ}-values in CZVEs of Σ33 GB cracks with varying impurity coverage, θ.

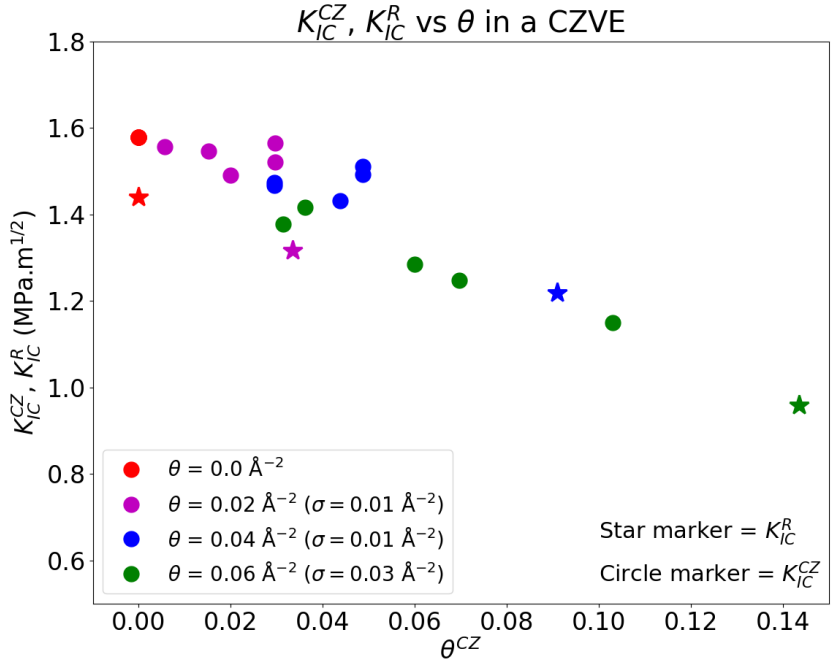

Fig. S11. K_{IC}^{CZ}-values in CZVEs of Σ43 GB cracks with varying impurity coverage, θ.

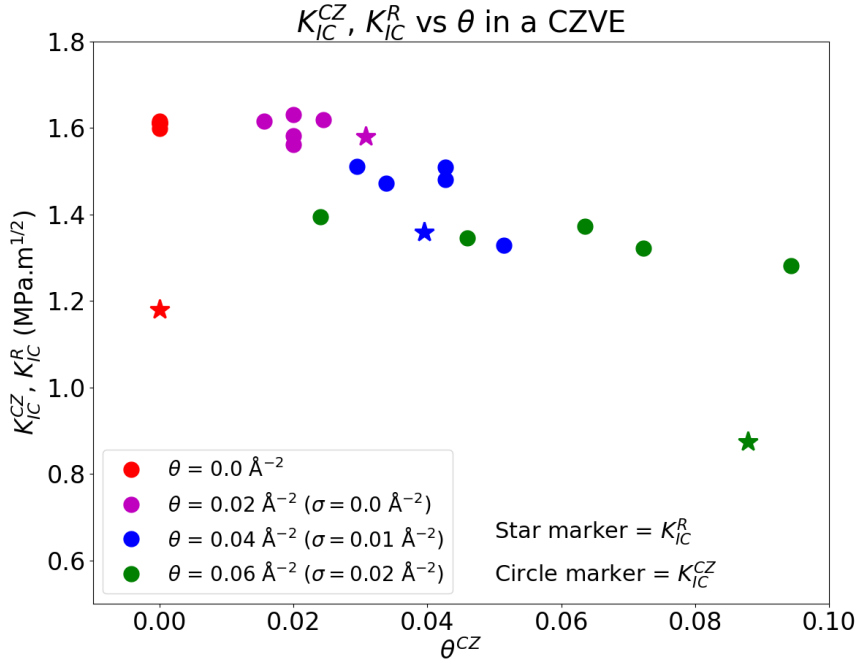

Fig. S12. K_{IC}^{CZ}-values in CZVEs of Σ51 GB cracks with varying impurity coverage, θ.

REFERENCES

1. G. C. Sih, P. Paris, and G. Irwin, "On cracks in rectilinearly anisotropic bodies," Int. J. Fract. Mech. **1**, 189–203 (1965).
2. G. Sih and H. Liebowitz, "Fracture: An Advanced Treatise," Math. Fundamentals **2**, 68–188 (1968).
3. K. S. Cheung and S. Yip, "A molecular-dynamics simulation of crack-tip extension: the brittle-to-ductile transition," Model. Simul. Mater. Sci. Eng. **2**, 865 (1994).
4. P. Hiremath, S. Melin, E. Bitzek, and P. A. T. Olsson, "Effects of interatomic potential on fracture behaviour in single-and bicrystalline tungsten," Comput. Mater. Sci. **207**, 111283 (2022).